

Vector Magnetic Field Measurement of NOAA AR 10197 *

Hong-Fei Liang^{1,2,3}, Hai-Juan Zhao⁴ and Fu-Yuan Xiang⁵

¹ National Astronomical Observatories / Yunnan Observatory, Chinese Academy of Sciences, Kunming 650011; njuf2003@yahoo.com.cn

² Graduate School of Chinese Academy of Sciences, Beijing 100049

³ Yunnan Normal University, Kunming 650092

⁴ National Satellite Meteorological Center, China Meteorological Administration, Beijing 100081

⁵ Xiangtan University, Xiangtan 411105

Received 2005 September 29; accepted 2006 May 30

Abstract A set of two-dimensional Stokes spectral data of NOAA AR 10197 obtained by the Solar Stokes Spectral Telescope (S^3T) at the Yunnan Observatory are qualitatively analyzed. The three components of the vector magnetic field, the strength H , inclination γ and azimuth χ , are derived. Based on the three components, we contour the distributions of the longitudinal magnetic field and transverse magnetic field. The active region (AR) has two different magnetic polarities apparent in the longitudinal magnetic map due to projection effect. There is a basic agreement on the longitudinal magnetic fields between the S^3T and SOHO/MDI magnetograms, with a correlation coefficient $\rho_{Bl} = 0.911$. The transverse magnetic field of the AR has a radial distribution from a center located in the southwest of the AR. It is also found that the transverse magnetic fields obtained by Huairou Solar Observing Station (HRSOS) have a similar radial distribution. The distributions of transverse magnetic field obtained by S^3T and HRSOS have correlation coefficients, $\rho_{Azimu} = 0.86$ and $\rho_{Bt} = 0.883$, in regard to the azimuthal angle and intensity.

Key words: line: profiles — sun: sunspots — sun: vector magnetic field — polarization

1 INTRODUCTION

It is well-known that strong magnetic fields of a few thousand Gauss exist in large sunspots and that they play a significant role in solar activities such as flares, filaments, sunspots, and CMEs. For understanding the structure and dynamics of sunspots, reliable measurement of the vector magnetic field in the solar photosphere, is necessary, for example, the Zeeman-induced polarization spectral lines are usually used to recover the form of the vector magnetic field in the photosphere (Skumanich & Lites 1987). Spectropolarimetry is one of the most useful instruments that deal with the solar magnetic field (del Toro Iniesta & Lopez Ariste 2003). Huge amounts of data of the magnetic field provided by advanced instruments compel solar researchers to develop or improve on more readily available and fast numerical solutions of the radiative transfer equation. The inversion method of Auer et al. (1977a, b) can give an estimation of the average magnetic field within the line forming region by assuming the Milne-Eddington model. An improved method can extract further information on the magnetic field gradient (Landi Degl'Innocenti & Landi Degl'Innocenti 1977). Using nonlinear least-squares algorithm, Skumanich et al. (1987) developed an inversion method to

* Supported by the National Natural Science Foundation of China.

produce routine maps of vector magnetic field. On the other hand, Ruiz Cobo & del Toro Iniesta (1994) obtained stratification velocities and a three-dimension magnetic structure of sunspot via Stokes profile analysis.

In the past few decades, many instruments have been built and developed world-wide to measure the vector magnetic field. These instruments can be divided into two kinds according to their observational technique and data reduction. One is the filtered type of measuring polarization in several fixed position of a spectral line profile, such as the Marshall Space Flight Center magnetograph (Hagyard et al. 1985) and the Huairou Solar Station vector magnetograph (Bao & Zhang 1998; Zhang & Bao 1998). The vector magnetic field \mathbf{B} is determined by comparing the measured polarizations with the theoretical ones based on some model of solar atmosphere (Semel et al. 1991). The well-known problem, magnetic saturation, produces measurement errors which limits the use of spectral data. The other is the spectral type that derives the magnetic field vectors from the full Stokes spectral line profiles, such as the Haleakala Stokes Polarimeter (Mickey 1985), the Advanced Stokes Polarimeter (Lites et al. 1993), THEMIS (Rayrole & Mein 1993) and the Solar Stokes Spectrum Telescope (hereafter S^3T) (Qu et al. 2001). Analysis of the spectral data provided by the spectropolarimeter is a powerful tool in finding the magnetic field structure of sunspots as well as the filtered type magnetograph. Furthermore, the magnetic helicities in the sunspot are often calculated based on the vector magnetograms by assuming a linear force-free field (Wang 1996; Zhang et al. 1999, 2001, 2002; Kim et al. 2002).

The S^3T can obtain simultaneously the full Stokes spectra of the two selected magneto-sensitive lines, Fe I 6301.5 Å (Lande factor $g_{\text{eff}} = 1.67$) and Fe I 6302.5 Å (Lande factor $g_{\text{eff}} = 2.5$). Through the Fourier transformation of the Stokes spectra data, the Stokes parameters I , Q , U and V can be demodulated (Qu et al. 2001). Fitting the Stokes profiles of I , Q , U and V , we derived spatial distributions of the three components of the vector magnetic field, magnetic field strength H , inclination γ , and azimuth χ . In this paper, we select a set of two-dimensional Stokes spectral data of NOAA AR10197 obtained by S^3T to measure the vector magnetic field in the sunspots.

2 OBSERVATIONS AND DATA REDUCTION OF NOAA AR 10197

Data provided by SOHO MDI show the evolution of the sunspot in NOAA AR10197. On November 13, 2002, the AR appeared in the east limb, at N25E90. Carried along by the sun's rotation, the AR moved from east to west. On November 19–20, it was located near the solar disk center and showed itself as a positive sunspot on the MDI magnetogram. The AR disappeared at the west limb on November 26.

On November 17, the AR was located at N25, E33. It was scanned by S^3T (Qu et al. 2001, 2005) with Fe I 6301.5 Å and Fe I 6302.5 Å, a pair of lines which are sensitive to the Zeeman effect, at the Yunnan Observatory, from 02:46 UT to 02:53 UT on November 17. The S^3T recorded 2D Stokes spectra of the AR by using a scanning technique with a step size of $4.5''$. Here, the measurement step are $0.5''$ (we take a point for every five step in this paper) along the slit and $15 \text{ m}\text{\AA}$ along the dispersion direction. The seeing was estimated to be around 2.0 arcsecond (Qu et al. 2001). During a scan, the scan step may vary somewhat due to the response of the electromotor and control system of S^3T . So, one image in the starting position and one in the end position are collected, to determine accurately the scan region and scan steplength, then from the length of the scanned region and the number of scanning steps, an average steplength is calculated. AR10197 is scanned by 14 steps and the scanned region is about 58 arcsecond in length from east to west. So the average steplength is $\frac{58}{14-1} = 4.5$ arcsecond. Figure 1 shows the scanning direction and the starting and end positions.

The S^3T is a complicated optical instrument composed of a primary mirror, a second mirror, a corrector, a reflector, a grating and a CCD (Qu et al. 2001). Some substantial errors are known to occur during the vector measurements. The imperfection and mis-alignment of the wave-plate and the prism would result in crosstalk among the measured Stokes I , Q , U and V . When the telescope pointed to the sun, the stress on the entrance window will induce an additional polarization source. Because of some scattered light due to multiple reflection and stray light due to light leakage in the spectrograph, an offset vector will be acquired by the shutting of the slit jaw. To obtain high precision measurements, a polarization calibration is introduced to eliminate the interference stripes produced by the imperfection of the rotating wave-plate and the following optics in the Stokes vector. By demodulating the calibrated intensity via Fourier Transformation,

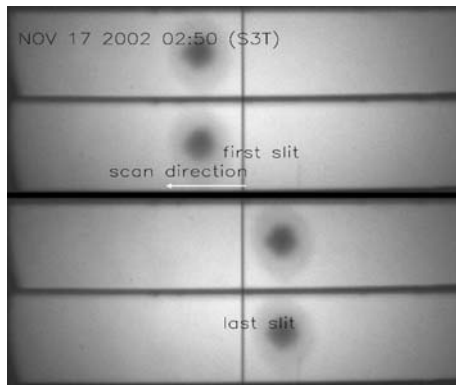


Fig. 1 Scanning position of AR 10197. The upper panel shows the first scanning position of the slit (02:46 UT), the lower panel, the last position (02:53 UT).

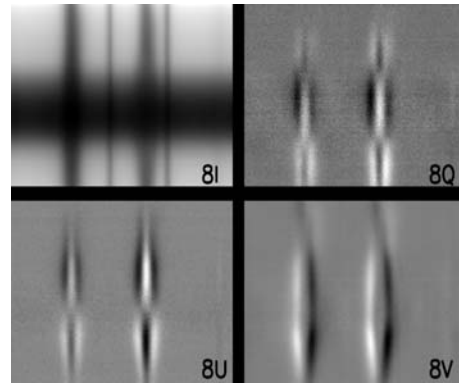


Fig. 2 Stokes spectra at the 8th scanning slit position.

the Stokes polarization components I , Q , U and V are derived (Qu et al. 2001). An example of the demodulated Stokes profiles is shown in Figure 2.

3 THE VECTOR MAGNETIC FIELD OF THE SUNSPOT IN AR 10197

Assuming that the entire atmosphere of the line forming region is a layer of constant physical parameters including the line source function S_l , magnetic field strength H , and inclination γ , etc., we use the formally integrated solution of the transfer equations for the polarized radiation (Landi Degli' Innocenti & Landi Degli' Innocenti 1985; Lites et al. 1988),

$$\mathbf{I}(\tau_c = 0) = \int_0^{\tau_c} \exp\left[-\mathbf{K} \frac{\tau}{\mu r_0}\right] \frac{\mathbf{j}}{\mu r_0} d\tau + \exp\left[-\mathbf{K} \frac{\tau_c}{\mu r_0}\right] \mathbf{I}(-\tau_c), \quad (1)$$

to fit the four Stokes profiles, and then obtain the values of the magnetic field strength H , azimuth χ , and inclination γ . In Equation (1), τ_c , \mathbf{K} , μ , r_0 , and \mathbf{j} are, in turn, the continuum optical depth, absorption matrix, cosine of heliocentric angle, reciprocal of the line strength parameter η_0 , and the emission vector. Figure 3 compares the four observational Stokes profiles and the corresponding synthetic profiles, showing that the observed and synthetic profiles are in good agreement with each other.

By fitting the 2D scanned data of the AR, we demodulated 2D distributions of the parameters of the magnetic field, such as the magnetic field strength H , azimuth χ , and inclination γ . Figure 4 shows the distribution of H where the contour lines basically circle around the sunspot. The maximum magnetic field strength is about 2100 G and is located some distance to the south of the center of the umbra. It should be mainly caused by the scattered light. A limb-darkening function (Pierce & Slaughter 1977) indicates that the continuum intensity dropped off quickly beyond the solar limb. With the limb-darkening, the northeast part of the AR is darker than the southwest and the observed umbra deviates from the real one toward the solar limb. Correspondingly, the maximum of the magnetic field strength deviates from the observed umbra toward the solar disk center. The field strength decreases steadily from the peak to about 1400 G at the interface of the umbra and penumbra, and to about 400 G at the edge of the sunspot. The rate of decrease is different in different directions, being larger in the southwestern than the northeastern direction.

From the magnetic field intensity H , inclination γ and azimuth χ , we can calculate the longitudinal and transverse magnetic fields of the AR as shown in Figure 5. We resolve the 180° ambiguity of azimuth χ by the method described by Canfield et al. (1993). In Figure 5, the longitudinal field is marked by the contour lines, and the transverse field, by the arrows which follow a radial pattern, with maximum about 1600 G at the center of the umbra. Figure 6 shows the Fe I 5324 Å image overlaid with the transverse magnetic field obtained by the Huairou Solar Observing Station near Beijing (HRSOS) on 2002 November 17 at 02:34 UT

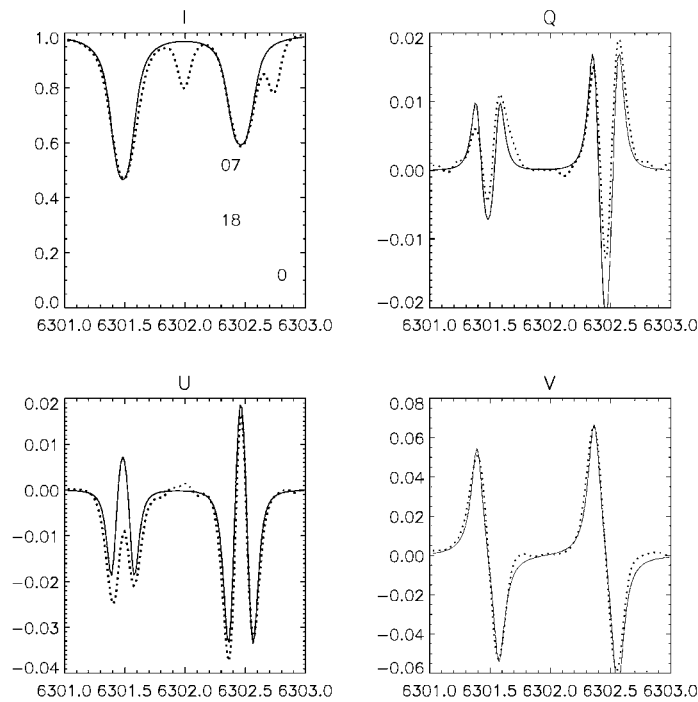


Fig. 3 Comparison of the observational Stokes I , Q , U , V (dotted lines) and the corresponding synthetic profiles (solid lines).

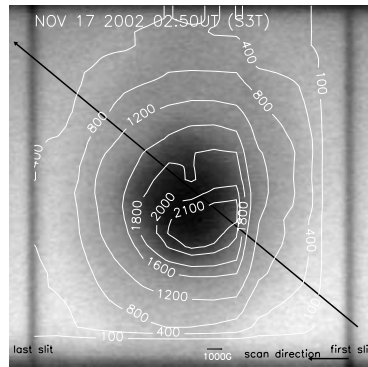


Fig. 4 White light image of the sunspot overlaid with contours of magnetic field strength (in Gauss).

(Ai & Hu 1986; Zhang et al. 2003), near the time of the S^3T observation (02:50 UT). Each pixel stands for $0.35'' \times 0.35''$ in the Huairou magnetogram (HRM) and $4.5'' \times 2.5''$ in S^3T magnetogram. To bring out the contrast, we resize the HRM magnetogram to $4.5'' \times 2.5''$ per pixel by linear interpolation. It is found that two magnetograms are basically consistent with each other in regard to the transverse field. The transverse field of HRM follows almost a radial distribution, too. The HRM and S^3T transverse magnetic fields are compared in regard to the azimuthal angle in Figures 7 and in regard to the intensity in Figure 8. The linear fit in Figure 7 is $Y = 12.6 + 0.88X$ with a correlation coefficient of $\rho_{Azimu} = 0.86$. The linear fit in Figure 8 is $Y = 39.5 + 0.965X$ with a correlation coefficient of $\rho_{Bt} = 0.883$. The two correlation

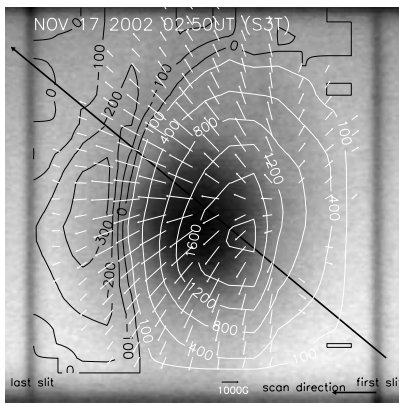


Fig. 5 White light image of the sunspot overlaid with contours of longitudinal magnetic field. The transverse magnetic field is indicated by the white arrows.

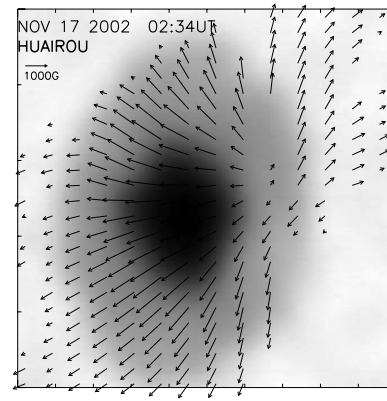


Fig. 6 Fe I 5324 Å image overlaid with the transverse magnetic field (black arrows). The field-of-view is $60'' \times 60''$. North is up, west to the right.

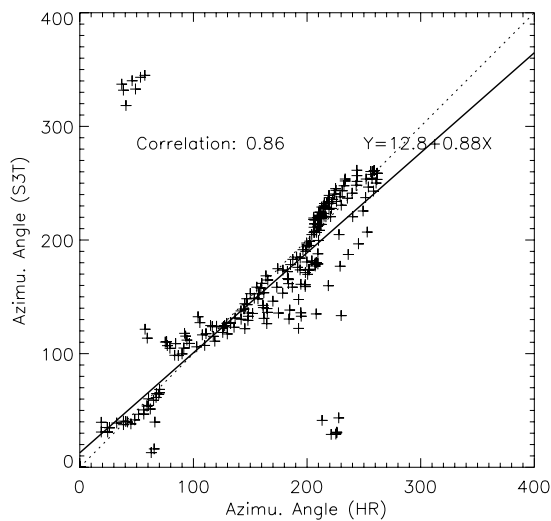


Fig. 7 Correlation between the azimuthal angles of the transverse magnetic field observed by S^3T and HRSOS.

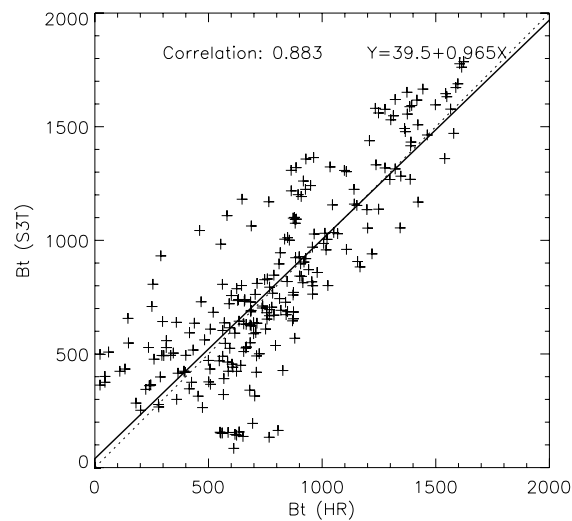


Fig. 8 Correlation between the intensities of the transverse magnetic field observed by S^3T and HRSOS.

coefficients indicate that there is a strong correlation between the transverse magnetic fields obtained by S^3T and HRSOS.

The contours show that the sunspot is made up of two regions of different magnetic polarities, and the western region is twice in area as the eastern one. The maximum of the western region (located to the southwest of the umbra) is about 2000 G; that of the eastern region is much less at about 300 G. The distribution of the longitudinal magnetic field is similar to that in the SOHO MDI magnetogram at 03:15:30 UT (near the time (02:50 UT) of the S^3T observation), as is shown in Figure 9. Here, the MDI magnetogram is overlaid with the S^3T contours of the longitudinal field. The outline of MDI magnetogram is seen to be in near agreement with the S^3T contours. To facilitate description, in the following B_{MDI} and B_{S^3T} will denote the longitudinal magnetic field obtained by MDI and S^3T , respectively. The large positive region in the

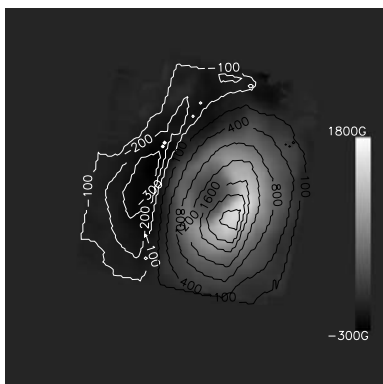


Fig. 9 SOHO MDI magnetogram (03:15:30 UT on 2002 November 17) overlaid with the contours of the longitudinal magnetic field calculated on the basis of S^3T Stokes spectra (02:50 UT on 2002 November 17). The field-of-view of the MDI magnetogram is $100'' \times 100''$. North is up, west to the right

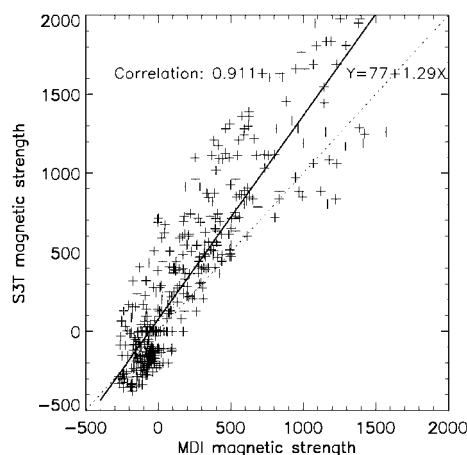


Fig. 10 Relationship between the two measured values of the longitudinal magnetic field strength (in units of Gauss) obtained by SOHO/MDI and S^3T . The line, $y = 77 + 1.29x$, represents a linear fit.

southwest is the major part of the AR, the negative region in the northeast being very small. The maximum (absolute value of the longitudinal field) of the latter is much less than that of the former. Different from our result, B_{MDI} is less than 300 G, very small in the center of the AR. Now, it is known that a correlation exists between the field strength and the continuum intensity: darker regions have stronger fields (Lites et al. 1991; Liu & Norton 2001). The magnetic field strength in the umbra should be the largest in the sunspot. Of course, the maximum of the longitudinal magnetic field may be separate from the maximum of the magnetic field strength, if the zero inclination ($\gamma = 0$) is not located at the center of the umbra. Even so, the longitudinal magnetic field at the center of the umbra can never be a minimum over the whole sunspot. The weaker magnetic strength of the umbra in the MDI magnetogram is mainly caused by saturation, which causes the flux in the MDI magnetogram to be no more than a few hundred Gauss in the umbrae. It has been understood that the saturation is a result of the right and left circular polarized line profiles moving beyond the wavelength sampling range of the filtergrams due to large magnetic fields and/or larger velocities (Liu & Norton 2001). The longitudinal magnetic field derived here decreases gradually, and no minimum appears at the center of the umbra.

As previously discussed, the longitudinal magnetogram obtained by S^3T is similar to the SOHO MDI magnetogram. The outline of MDI magnetogram is in rough agreement with the contours of B_{S^3T} except in the center of the umbra where B_{MDI} is much smaller than B_{S^3T} . The difference should be caused by the magnetic saturation in the MDI observation. To compare the two magnetograms quantitatively, we delete the values in the center of the umbra where the B_{MDI} is meaningless. Now, the scale of the pixel is different in the two magnetograms, it is $4.5'' \times 2.5''$ per pixel in S^3T and $2'' \times 2''$ per pixel in MDI. So we expand the size of both magnetograms by linear interpolation to $1'' \times 1''$ per pixel. Figure 10 shows the correlation between the B_{MDI} and B_{S^3T} reduced to in the same scale. It shows that the MDI values are generally smaller than the S^3T values. A linear fit between the two is represented by the solid line $Y = 77 + 1.29X$, with a correlation coefficient $\rho_{BI} = 0.911$, so indicating strong correlation. The distributions of B_{S^3T} and B_{MDI} are similar.

4 DISCUSSION AND CONCLUSIONS

By fitting several hundreds of Stokes profiles of NOAA AR10197, we obtain distributions of the three components, i.e., the strength H , inclination γ and azimuth χ . The field strength contours basically circle around the sunspot and the maximum strength near the center of the umbra is about 2100 G. The AR at N25E33, is

some 40 degrees from the solar disk center. Under the projection the maximum of the longitudinal magnetic field H is not located in the center of the umbra, rather, to the southwest of the center. The transverse magnetic field follows a radial pattern. It is also found that there are similar distributions of transverse magnetic field in the HRM magnetogram of the same day. The contours show that the AR has a mixed polarity that is apparent in the magnetogram. By comparing the longitudinal magnetic field in our result with the SOHO MDI magnetogram, we find that they are similar except in the umbra: the MDI field is much weaker there, but this is mainly caused by magnetic saturation. The saturation renders problematic MDI umbral values of only a few hundred Gauss.

The distributions of the transverse magnetic fields obtained by HRSOS and S^3T are similar, with strong correlation coefficients, $\rho_{Azimu} = 0.86$ and $\rho_{Bt} = 0.883$. By comparing the values of B_{MDI} and B_{S^3T} for the same spatial locations, we find the two magnetograms are strongly correlated. Furthermore, the value of B_{\parallel} is smaller in the MDI than the S^3T magnetogram. The good linear relationship between B_{MDI} and B_{S^3T} indicates that B_{S^3T} and B_{MDI} of the two magnetograms have a similar distribution with each other.

Acknowledgements The authors would like to thank the anonymous referee for the useful and helpful comments on the manuscript. We also express our thanks to Prof. Li K.J. for his careful reading and helpful suggestion. We also thank Prof. Qu Z. Q., Zhang X. Y. and other S^3T staff of Yunnan Observatory, and Ms. Wang G. P. and other HRSOS staff at National Astronomical Observatories, CAS, for their help to supply the spectral data.

References

- Ai G. X., Hu Y. F., 1986, Publ. Beijing Astron. Obs., 8, 1
 Auer L. H., Heasley J. N., House L. L., 1977a, Solar Physics, 55, 47
 Auer L. H., Heasley J. N., House L. L., 1977b, ApJ, 216, 531
 Bao S., Zhang H., 1998, ApJ, 496, L43
 Canfield R. C., de La Beaujardiere J. F., Fan Y. H. et al., 1993, ApJ, 411, 362
 Hagyard M. J., Cumings N. P., West E. A., 1985, In: C. De Jager, Chen Biao, eds., Proceedings of Kunming Workshop on Solar Physics and Interplanetary Traveling Phenomena, Beijing: Science Press, p.204
 Kim J. S., Zhang H. Q., Kim J. S. et al., 2002, ChJAA, 2, 81
 Landi Degl'Innocenti E., Landi Degl'Innocenti M., 1977, Solar Physics, 31, 299
 Landi Degl'Innocenti E., Landi Degl'Innocenti M., 1985, Solar Physics, 97, 239
 Lites B. W., Skumanich A., Rees D. E. et al., 1988, ApJ, 330, 493
 Lites B. W., Bida T. A., Johannesson A. et al., 1991, ApJ, 373, 683
 Lites B., Elmore D. F., Seagraves P. et al., 1993, ApJ, 418, 928
 Liu Y., Norton A. A., 2001, MDI Measurement Errors: The Magnetic Perspective SOI-Technical Note 01-144, Published on the website <http://soi.stanford.edu/general/TechNotes/01.144/TN01-144.pdf>
 Mickey D. L., 1985, Solar Physics, 97, 223
 Pierce A. K., Slaughter C. D., 1977, Solar Physics, 51, 25
 Qu Z. Q., Zhang X. Y., Chen X. K. et al., 2001, Solar Physics, 201, 241
 Qu Z. Q., Wang S., Xu C. L. et al., 2005, ChJAA, 5, 426
 Rayrole J., Mein P., 1993, Proc. IAU Colloq., 141, 170
 Ruiz Cobo B., del Toro Iniesta J. C., 1994, A&A, 283, 129
 Semel M., Mouradian Z., Soru-Escout M. et al., 1991, Active regions, sunspots and their magnetic fields, in Solar Interior and Atmosphere, eds., A. Cox, W. Livingston, M. Matthews, Tucson: The Univ. of Arizona Press, p.844
 Skumanich A., Lites B. W., 1987, ApJ, 322, 473
 del Toro Iniesta J. C., Lopez Ariste A., 2003, A&A, 412, 875
 Wang J. X., 1996, Solar Physics, 163, 319
 Zhang H. Q., Bao S. D., 1998, A&A, 339, 880
 Zhang H. Q., Bao S. D., 1999, ApJ, 519, 876
 Zhang H. Q., 2001, MNRAS, 326, 57
 Zhang H. Q., 2002, MNRAS, 332, 500
 Zhang H., Labonte B., Li J. et al., 2003, Solar Physics, 213, 87